

Plant Cytokinesis Is Orchestrated by the Sequential Action of the TRAPP^{II} and Exocyst Tethering Complexes

Katarzyna Rybak,¹ Alexander Steiner,¹ Lukas Synek,² Susan Klaeger,³ Ivan Kulich,⁴ Eva Facher,^{5,6} Gerhard Wanner,⁶ Bernhard Kuster,³ Viktor Zarsky,^{2,4} Staffan Persson,^{7,8} and Farhah F. Assaad^{1,*}

¹Botany, Technische Universität München, 85354 Freising, Germany

²Institute of Experimental Botany, Academy of Sciences of the Czech Republic, 165 02 Prague 6, Czech Republic

³Chair for Proteomics and Bioanalytics, Technische Universität München, 85354 Freising, Germany

⁴Department of Experimental Plant Biology, Faculty of Science, Charles University, 128 44 Prague 2, Czech Republic

⁵Department Biologie I, Ludwig-Maximilians Universität, Systematische Botanik und Mykologie, 80638 Munich, Germany

⁶Department Biologie I, Ludwig-Maximilians Universität, 82152 Planegg-Martinsried, Germany

⁷Max-Planck-Institut für Molekulare Pflanzenphysiologie, 14476 Potsdam, Germany

⁸ARC Centre of Excellence in Plant Cell Walls, School of Botany, University of Melbourne, Parkville, VIC 3010, Australia

*Correspondence: farhah@wzw.tum.de

<http://dx.doi.org/10.1016/j.devcel.2014.04.029>

SUMMARY

Plant cytokinesis is initiated in a transient membrane compartment, the cell plate, and completed by a process of maturation during which the cell plate becomes a cross wall. How the transition from juvenile to adult stages occurs is poorly understood. In this study, we monitor the *Arabidopsis* transport protein particle II (TRAPP^{II}) and exocyst tethering complexes throughout cytokinesis. We show that their appearance is predominantly sequential, with brief overlap at the onset and end of cytokinesis. The TRAPP^{II} complex is required for cell plate biogenesis, and the exocyst is required for cell plate maturation. The TRAPP^{II} complex sorts plasma membrane proteins, including exocyst subunits, at the cell plate throughout cytokinesis. We show that the two tethering complexes physically interact and propose that their coordinated action may orchestrate not only plant but also animal cytokinesis.

INTRODUCTION

Cytokinesis is the partitioning of the cytoplasm following nuclear division. In plants, this occurs in a transient membrane compartment called the cell plate. Following its biogenesis and expansion, the cell plate is inserted into the lateral walls of the parent cell. A number of changes in the properties and composition of the plate occur thereafter, and insertion thus appears to trigger the maturation of the cell plate into a cross wall. Live imaging of asymmetric cytokinetic events has documented a dramatic change in the growth dynamics of nascent cell plates upon anchoring to one side of the cell: whereas cell plate movements prior to insertion could best be described as tentative, cell plate growth becomes rapid and highly directional upon connecting with a lateral wall (Cutler and Ehrhardt, 2002). Similarly, time-lapse images of *Tradescantia* stamen hair cells show fluid and

wrinkled cell plates becoming stiff and flat after insertion into the parent cell walls (Mineyuki and Gunning, 1990). This difference in appearance requires cellulose synthesis (Mineyuki and Gunning, 1990), and immunohistochemistry has in fact shown that cellulose is a major component of mature cross walls (Samuels et al., 1995). This is in contrast to cell plates, in which the principle luminal polysaccharide is callose (Samuels et al., 1995; Seguí-Simarro et al., 2004). The abundance of other cell wall polysaccharides, including pectins and xyloglucans, also differs between cell plates and cross walls (Moore and Staehelin, 1988). Although it is apparent that the composition of cell plate membranes and polysaccharides changes as this juvenile compartment matures into a cross wall, the mechanisms that coordinate these transitions remain unclear.

In contrast to plants, cytokinesis in animal cells occurs by means of a ring of actin and myosin that contracts to pinch a cell in two (Neto and Gould, 2011). This process requires extensive cell-surface expansion, which is achieved by the delivery of membranes from the recycling endosome to the cleavage furrow (Robinett et al., 2009). The completion of animal cytokinesis, via a process referred to as abscission, requires the delivery of secretory vesicles to a scaffold assembled at the midbody (Gromley et al., 2005). The regulation of the transition between furrow ingression and abscission is poorly understood. Thus, in both plant and animal cells, cytokinesis requires the regulation in time and space of a series of successive steps, and in neither kingdom have the underlying mechanisms been elucidated.

Although plants and animals adopt different strategies for cytokinesis, a number of conserved molecular components are shared. These include Rab GTPases and other factors that are required for vesicle tethering. Tethering refers to the initial contact between donor and recipient membranes and represents a highly selective trafficking step that precedes and facilitates vesicle docking and fusion (see Thellmann et al., 2010, and references therein). The *Arabidopsis* Rab-A subfamily of small GTPases is the only one that labels the cell plate throughout cytokinesis (Chow et al., 2008). Similarly, the orthologous Rab11 class is the only one that has been shown to be required for and present throughout animal cytokinesis (Yu et al., 2007).

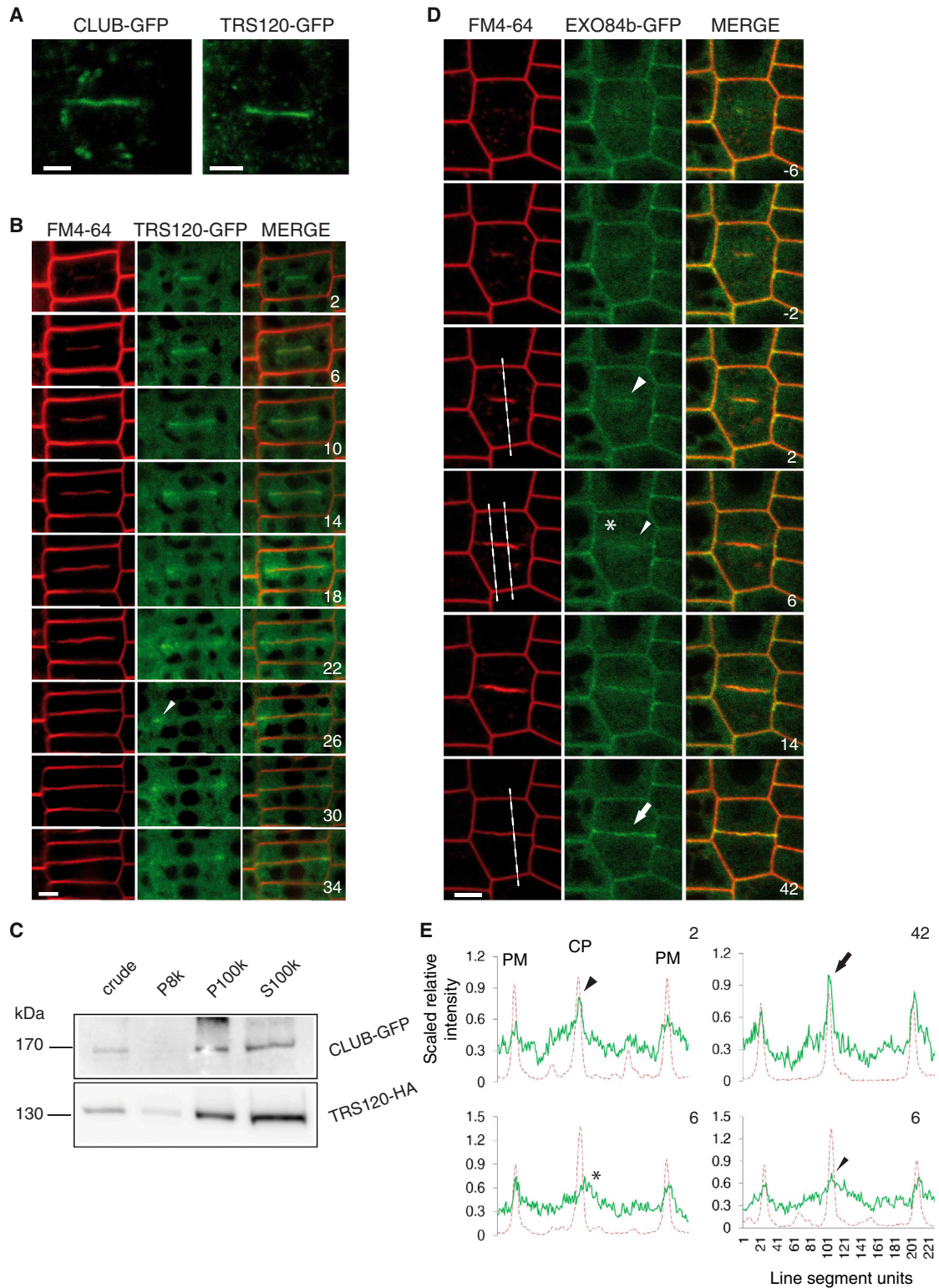


Figure 1. Localization Dynamics of TRAPP^{II} and Exocyst Gene Fusions

(A) Cell plate localization of P_{UBQ}::CLUB-GFP (left) and P_{TRS120}::TRS120-GFP (right).

(B and D) Time lapses of P_{TRS120}::TRS120-GFP (B) and P_{EXO84b}::EXO84b-GFP (D) with FM4-64 are shown, with minutes indicated in the right panel. The 0 min time point corresponds to cell plate initiation. Arrowhead in (B) points to leading edge of cell plate.

(C) Cell fractionation showing that CLUB-GFP and TRS120-HA can be detected in both the membrane (P100k) and soluble (S100k) fractions.

(legend continued on next page)

Two distinct tethering complexes, the transport protein particle II (TRAPP_{II}) and exocyst, have been implicated in cytokinesis in both the plant and animal kingdoms (McMichael and Bednarek, 2013; Neto and Gould, 2011). The yeast TRAPP_{II} complex acts as a guanine nucleotide exchange factor for Rab GTPases and is required for intra- and post-Golgi traffic; it consists of the hexameric TRAPP_I complex and of three additional subunits (Trs65, Trs120, and Trs130; Yu and Liang, 2012). All subunits but one (Trs65) are conserved in plants (Thellmann et al., 2010). The exocyst is a conserved octameric complex required for polarized secretion (reviewed in Heider and Munson, 2012). The *Arabidopsis* genome encodes single or multiple isoforms of all exocyst subunits (Sec3, Sec5, Sec6, Sec8, Sec10, Sec15, Exo70, and Exo84; Cvrckova et al., 2001; Synek et al., 2006).

The *Arabidopsis* TRAPP_{II} complex was first identified in a screen for cytokinesis-defective mutants (Jaber et al., 2010); mutation at the *CLUB* locus gave rise to seedlings with multinucleate cells, cell wall stubs as well as an amorphous, club-shaped overall appearance, hence the name (Söllner et al., 2002). Positional cloning identified *CLUB* as a homolog of the yeast Trs130 TRAPP_{II}-specific subunit (Jaber et al., 2010). The two conserved *Arabidopsis* TRAPP_{II} subunits, CLUB/AtTRS130 and AtTRS120, have been shown to be required for cell plate formation (Jaber et al., 2010; Thellmann et al., 2010; Qi et al., 2011), but their localization dynamics during cytokinesis has not been determined to date. A number of studies have addressed the role of the exocyst in plant cytokinesis. The EXO70A1 and EXO84b exocyst subunits localize to nascent cell plates and postcytokinetic cross walls and were found to be involved in cytokinesis (Fendrych et al., 2010). The SEC6 exocyst subunit interacts with the Sec1/Munc18 protein KEULE, and pollen-rescued *sec6* mutant embryos have been reported to have a canonical *keule*-like phenotype, with multinucleate cells and cell wall stubs (Wu et al., 2013). However, such cytokinesis defects were not observed in embryo lethal *sec3a* exocyst mutants of *Arabidopsis* (Zhang et al., 2013). In brief, the literature on the role of the exocyst in cell plate formation is internally inconsistent, and there is no clear consensus as regards the cell plate localization of the exocyst throughout cytokinesis.

The finding that both the TRAPP_{II} and exocyst tethering complexes are required for plant cytokinesis is intriguing. The TRAPP_{II} complex is functionally related to Rab-A but not Rab-D family members in *Arabidopsis* and colocalizes with Rab-A1c (Qi et al., 2011; Qi and Zheng, 2011). It is thereby thought to label *trans*-Golgi network (TGN) compartments. By contrast, the exocyst partitions between the cytoplasm and the plasma membrane, where it forms distinct, transient foci (Fendrych et al., 2013; Zhang et al., 2013). This raises the question as to whether the cell plate may have a mosaic identity, consisting simultaneously of both TGN and plasma membrane components. An alternative hypothesis would postulate a sequential identity for the cell plate as it undergoes initiation, biogenesis, expansion, and maturation. In this study, we simultaneously

monitor the TRAPP_{II} and exocyst complexes throughout cytokinesis. Our data support a sequential identity for the cell plate. In addition, we show that the TRAPP_{II} complex regulates the localization of the exocyst at the cell plate and that the two complexes physically interact. We present a model for the sequential yet overlapping, coordinated action of the TRAPP_{II} and exocyst complexes in cytokinesis.

RESULTS

The Appearance of the TRAPP_{II} and Exocyst Complexes at the Cell Plate Is Predominantly Sequential, with a Brief Overlap at the Onset and End of Cytokinesis

We first set out to elucidate the localization dynamics of TRAPP_{II} and exocyst subunits throughout cytokinesis. CLUB/AtTRS130 and AtTRS120 GFP fusions, expressed under the control of ubiquitin and/or native promoters, were shown to be functional (Figures S1A–S1C available online) and found to reside on the cell plate (Figures 1A and 1B). As CLUB/AtTRS130 and AtTRS120 show very similar localization dynamics at the cell plate (Figure S2), we continued predominantly with TRS120 gene fusions, which yielded a brighter signal. TRS120-GFP appeared at the cell equator at the onset of cytokinesis and labeled the cell plate throughout cytokinesis, disappearing after cell plate insertion into the lateral cell walls (Figure 1B; Movie S1). TRAPP_{II} gene fusions appeared to localize in the cytoplasm as well as on membrane structures (Figure 1B; Figure S2); upon cell fractionation, CLUB-GFP and TRS120-hemagglutinin (HA) gene fusions were found in both the soluble and membrane fractions (Figure 1C). It thus appears that these subunits shuttle between the cytosol and endomembrane compartments. In contrast to the TRAPP_{II} subunits, EXO84b-GFP appeared at the cell equator at the onset and at the end of cytokinesis and labeled membranes associated with newly deposited cross walls after cytokinesis (Figure 1D; Movie S2; Fendrych et al., 2010). In expanding cell plates, peak EXO84b-GFP fluorescence was typically not at the cell plate, but rather present as a diffuse cloud around the plate; this was often observed in discontinuous patches of the cell plate (Figures 1D and 1E, 6 min time point; Figure S5D; Movie S2) and could be seen throughout the biogenesis and expansion phases of cytokinesis (Figure S1). The localization dynamics of different TRAPP_{II} and exocyst subunits did not appear to be due to overexpression of the fusion proteins and was robust over a considerable range of protein expression levels (Figures S1D–S1K; Movies S1, S2, and S3). Furthermore, different subunits of each complex behaved similarly (Figures 2A and 2B).

To better monitor the different stages of cytokinesis, we used a microtubule marker, mCherry-TUA5 (Gutierrez et al., 2009). The onset of cytokinesis is characterized by the assembly of the phragmoplast, which is a transient array of polar microtubules nucleated from spindle microtubules. A solid phragmoplast subsequently arises from lateral expansion of phragmoplast initials. As cells enter telophase, microtubules are translocated

(E) Line graphs, corresponding to panels shown in (D), depict scaled relative fluorescence intensity, with FM4-64 used to position the plasma membranes (PM) and cell plate (CP). The arrowhead at 2 min points to an initial signal at the cell plate, the arrow at 42 min points to peak signal at the cross wall. At 6 min the signal is more diffuse, with a cloud-like appearance on the left (asterisk) and weak signal at the cell plate on the right (arrowhead). Scale bars, 5 μ m. See also Figures S1 and S2 and Movies S1 and S2.

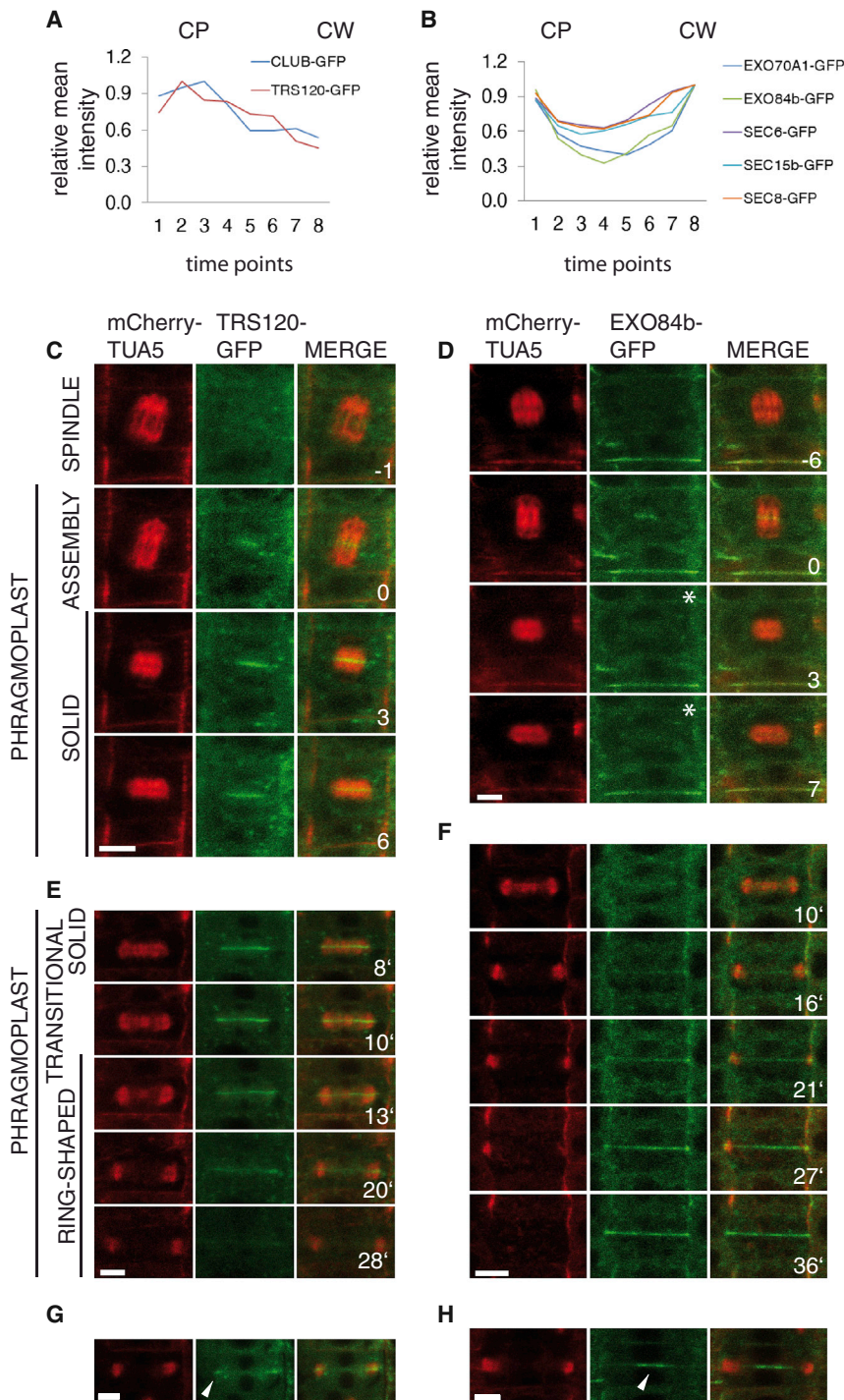


Figure 2. Localization of TRAPP11 and Exocyst Gene Fusions and Phragmoplast Microtubule Dynamics

(A and B) Mean signal intensity at the CP or cross walls (CW). The value 1.0 is set at maximal CP signal in (A) and maximal CW signal in (B). (A) TRAPP11 subunits show peak fluorescence at the cell plate and are absent at the cross wall. (B) All exocyst subunits monitored (SEC6, SEC8, SEC15b, EXO70A1, and EXO84b; Fendrych et al., 2010) follow a localization dynamics we refer to as “strong-weak/diffuse-strong.”

(C–H) Time lapses of $P_{\text{TRS120}}::\text{TRS120-GFP}$ (C and E) and $P_{\text{EXO84b}}::\text{EXO84b-GFP}$ (D and F) with mCherry-TUA5 are shown, with minutes indicated in the right panel.

(C and D) Anaphase-telophase transition. The 0 min time point corresponds to cell plate initiation. Star in (D) at 3 and 7 designates barely detectable, diffuse EXO84b-GFP cytosolic signal.

(E and F) Telophase. The time-lapse segments start at the solid phragmoplast stage, which occurs on average 8 min after cell plate initiation, hence the labeling 8', etc.

(G and H) Ring-shaped phragmoplast stage. Arrowhead in (G) points to leading edge of cell plate. Arrowhead in (H) points to first appearance of the exocyst subunit. The brief window in time shown in (G) and (H) was missed in the time lapses shown in (E) and (F). This is because the fluorescence was low and photobleaching extensive, such that time lapses were carried out with 4 min intervals. Scale bars, 5 μm .

See also Figure S2 and Movies S1, S2, and S3.

plast, TRS120-GFP relocated to the leading edges of the cell plate (Figure 2G; Figure S2B) and then gradually disappeared (Figure 2E; Figure S2B). The EXO84b-GFP fluorescence remained weak and diffuse until this time point (Figures 2F and 2H). Thereafter, the EXO84b-GFP signal gradually increased (Figure 2F; Figure S2C; Fendrych et al., 2010) to reach peak fluorescence throughout the cross wall as the phragmoplast disappeared (Figure 2F; Figure S2C).

An analysis of colocalization was undertaken with TRS120 and three exocyst subunits (SEC6, EXO70A1, and EXO84b) with different combinations of mCherry or monomeric red fluorescent protein (mRFP) and GFP tags. All three combina-

to the leading edges of the phragmoplast, giving rise to a ring-shaped phragmoplast (McMichael and Bednarek, 2013). TRS120-GFP and EXO84b-GFP first appeared at the cell equator at the phragmoplast assembly stage (Figures 2C and 2D; Figure S2). At the solid phragmoplast stage, however, TRS120-GFP fluorescence at the cell plate reached a peak (Figure 2C; Figure S2B), whereas the EXO84b-GFP signal became weak and diffuse (Figure 2D; Figure S2C). At the ring-shaped phragmo-

plasts yielded the same results (Figure 3A; Figure S3; data not shown). Whereas peak fluorescence of TRS120 was seen during cell plate formation, peak fluorescence of the exocyst subunit was associated with cross walls, where TRS120 was absent (Figures 3A and 3B). A brief overlap between the two tethering complexes could be seen not only at the onset of cytokinesis (Figure 3A, 0 min) but also as of a time point at which the TRS120 signal began to decrease at the cell plate and increase

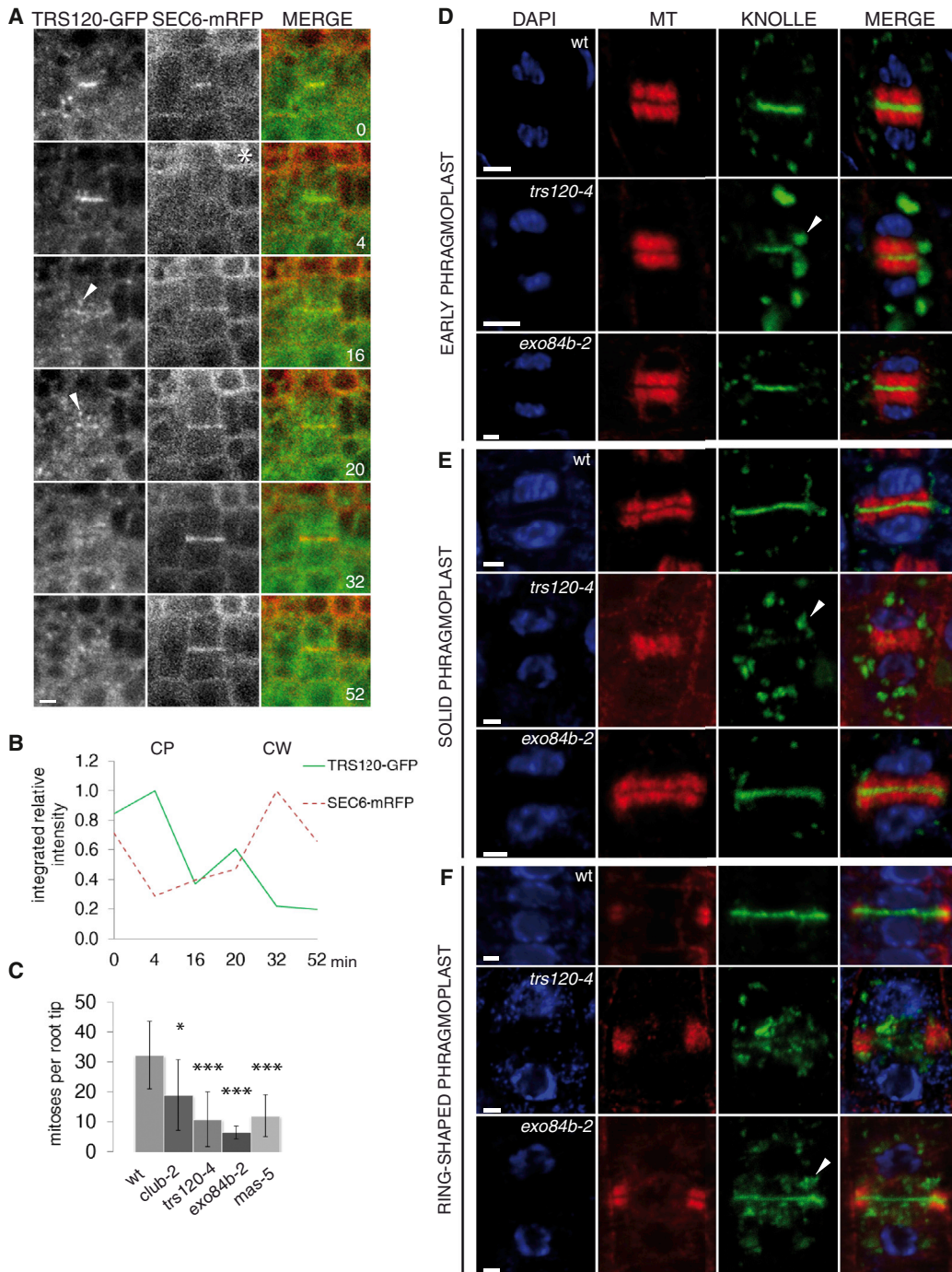


Figure 3. Colocalization of TRAPP11 and Exocyst Subunits as well as Cell Plate Biogenesis and Maturation in Wild-Type and Mutant Backgrounds

(A and B) Time lapse of $P_{UBQ}::TRS120$ -mCherry and $P_{35S}::SEC6$ -mRFP, with minutes indicated in the right panel. (A) z stack projections generated with a spinning disk confocal microscope. Star at 4 min designates barely detectable, diffuse SEC6-mRFP cytosolic signal. Arrowheads at 16 and 20 min point to TRS120 recycling from the cell plate. Scale bar, 5 μ m. Line graph (B) shows integrated signal intensity per unit area at the cell plate or cross wall, with peak signals set at 1.0.

(C) Mitotic index (mean \pm SD) of wild-type (WT) and mutant root tips. All mutants show a significantly lower mitotic index than the wild-type ($n > 15$, $*p \leq 0.01$ and $***p \leq 0.0001$; Student's t test).

(D–F) Antibody stains of root tips: DAPI/nucleus (blue), microtubules (MT, red), KNOLLE protein (green), and merge. The cell-cycle stage is indicated on the left and the genotype in the first column. Arrowheads point to large KNOLLE-positive compartments surrounding thin or absent cell plates in *trs120-4* (D–F) and surrounding telophase plates in *exo84b-2* (F). See text for a detailed description. Scale bars, 2 μ m.

See also Figure S3.

in intracellular compartments (Figure 3A, 16 min). Our analysis of SEC6 is discrepant with the findings of Wu et al. (2013), who describe a similar SEC6-GFP fusion as labeling cell plate membranes throughout cytokinesis, and of reorganizing to the leading edges at the end of cytokinesis. This discrepancy might be attributed to the fact that Wu et al. (2013) used tobacco BY2 protoplasts for localization. The consensus (based on this study, Fendrych et al., 2010, and Zhang et al., 2013) in meristematic cells of root tips and embryos is that the exocyst signal is weak during the solid phragmoplast stages.

Taken together, our data show that the appearance of the TRAPP^{II} and exocyst complexes was predominantly sequential. The overlap between the complexes occurred at two key transitions: during the phragmoplast assembly stage at the onset of cytokinesis, and at the late ring-shaped phragmoplast stage, which is concomitant with cell plate insertion into the lateral walls at the end of cytokinesis.

The TRAPP^{II} Complex Is Required for Cell Plate Biogenesis, and the Exocyst Is Required for Cell Plate Maturation

We next compared cell plate formation and maturation in TRAPP^{II} and exocyst mutants. TRAPP^{II} mutants of *Arabidopsis* are seedling lethal, whereas exocyst mutants range from gametophytic lethality to viability (see Supplemental Experimental Procedures), depending presumably on the degree of redundancy between paralogs. To compare TRAPP^{II} and exocyst mutant phenotypes of similar strength, we screened 54 insertion lines in exocyst subunits for strong cytokinesis defects (see Supplemental Experimental Procedures). The screen identified one exocyst mutant, *exo84b-2*, with a seedling lethal phenotype of roughly equal strength as TRAPP^{II} mutants in terms of growth and meristem dysfunction, and we therefore focused on it in this study. Wild-type and mutant root tips were stained with DAPI to determine nuclear stages and labeled with α -microtubule and α -KNOLLE antibodies to visualize phragmoplast microtubules and cell plate membranes, respectively (Figures 3C–3F). The stains revealed that the mitotic index of *exo84b-2* root meristems (Figure 3C) was significantly lower than that of TRAPP^{II} mutants ($p = 0.004$ for an average of *club-2* and *trs120-4*) and of other canonical cytokinesis-defective mutants such as *massue* (Thiele et al., 2009; $p = 0.002$ for *mas-5*), which made it difficult to obtain a large number of cytokinetic cells. Throughout the early-to-late solid phragmoplast stages, *trs120-4*, but not *exo84b-2*, mutants showed a defect in cell plate biogenesis (Figures 3D and 3E). Indeed, 84% of *trs120* and *club* cell plates were absent, patchy, thin, or incomplete ($n = 183$), whereas 92% of *exo84b-2* ($n = 48$) and 84% of wild-type ($n = 115$) cell plates appeared complete at this stage. Although *exo84b-2* mutants did not exhibit anomalies at the beginning of cytokinesis, they differed from the wild-type at the end of cytokinesis. In the wild-type, KNOLLE is actively removed from the cell plate as of the late ring-shaped phragmoplast stage, once the plate has fully expanded to reach the lateral walls. In *exo84b-2* mutants, KNOLLE prematurely appeared as a punctate stain at the cell plate, already at early ring-shaped phragmoplast stages (Figure 3F, arrowhead). This was also observed in *trs120-4* mutants, but, in this case, the solid and ring-shaped

phragmoplast stages did not considerably differ (compare Figure 3E with Figure 3F).

As cell plate formation was not impaired in *exo84b-2*, possible explanations for the premature removal of KNOLLE include impaired stability or maturation of the cell plate. We reasoned that impaired cell plate stability would result in incomplete cross walls and cell wall stubs. FM4-64 stains, however, failed to detect such defects in *exo84b-2* root meristems, even though stubs have been observed in leaf cells in this mutant, as have guard cells with incomplete ventral walls (Fendrych et al., 2010). As confocal microscopy cannot resolve small cell wall gaps, we applied focused ion beam/scanning electron microscopy (FIB/SEM), which allows for 3D reconstructions of high-resolution images of entire cells (Figure 4). FIB/SEM tomographic data sets failed to reveal reproducible cell wall defects in *exo84b-2* (Figure 4B; $n > 200$ cells), but detected frequent (33%, $n = 33$ cells) stubs and incomplete walls in *trs120-4* mutants (Figure 4C; Figure S4). Transmission electron microscopy (TEM) also failed to reveal reproducible cross wall defects in *exo84b-2* root tips (Figure 4E), but cross walls in *trs120-4* root tips occasionally resembled beads on a string (Figure 4F). In summary, antibody stains, FIB/SEM, and TEM revealed cell plate biogenesis defects in TRAPP^{II}, but not in *exo84b-2*, mutants.

To assess cell plate and cross wall maturation in *exo84b-2*, we carried out a survey with 13 different antibodies against cell wall polysaccharides, including callose, cellulose, xyloglucans, pectins, and α 1-acid glycoprotein (AGP) glycans (see Supplemental Experimental Procedures). We focused on methyl-esterified pectins (JIM7 antibody, Clausen et al., 2003), as this labeled the cell plate throughout cytokinesis (Figure 5A, wild-type, left panels), and on AGP glycans (LM14 antibody, Moller et al., 2008) as a good marker for nascent cross walls and mature cell walls. In *club-2* mutants there was almost no JIM7 signal at the cell plate (Figure 5A, middle panels). In *exo84b-2*, cell plate labeling was variable and was often ectopically detected on lateral walls and cross walls (Figure 5A, right panels; Figure 5B), which were rarely detected in the wild-type (Figure 5A, left panels; Figure 5B). In contrast to JIM7, which labeled the cell plate throughout cytokinesis, LM14 was predominantly seen on lateral walls and labeled cell plates only after insertion (as inferred from late ring-shaped phragmoplast microtubules having reached the outer edges of the cell) into the lateral walls in the wild-type (Figure 5C, left panels). In *club-2*, cell walls were often weakly labeled, and LM14-positive compartments were ectopically seen in the cytosol (Figure 5C, middle panels). In *exo84b-2*, the wall stains were somewhat punctate; telophase plates were often labeled to a greater extent than the wild-type, with little signal on lateral walls (Figure 5C, right panels). We conclude that the relative content of methyl-esterified pectins and AGP glycans was altered in the cell plates, cross walls, and lateral walls of both TRAPP^{II} and exocyst mutants.

The TRAPP^{II} Complex Is Required for Protein Sorting at the Cell Plate

We next asked whether the TRAPP^{II} complex is required for the targeting of the exocyst to the cell plate or plasma membrane, and whether, conversely, the exocyst regulates TRAPP^{II} localization. TRS120-GFP targeting to expanding cell plates did not

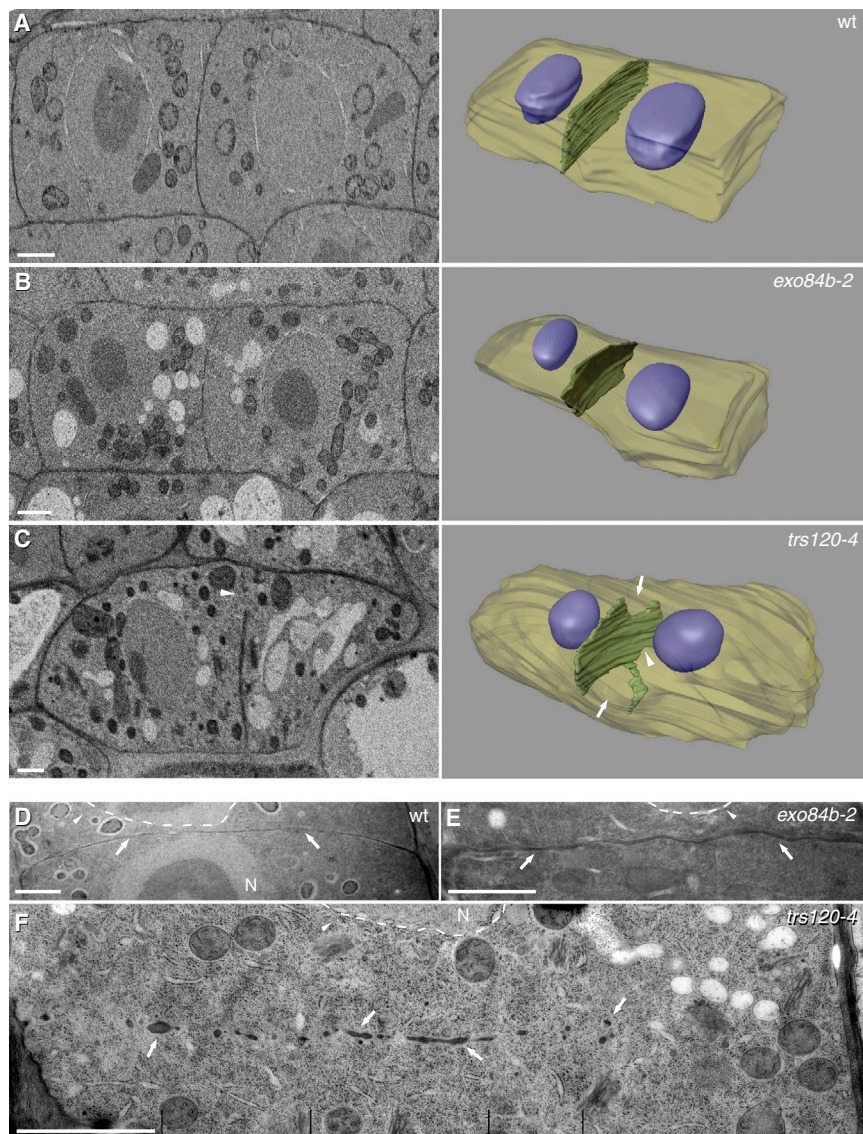


Figure 4. Electron Micrographs of High-Pressure Frozen, Freeze-Substituted 5-Day-Old Root Tips

Wild-type (A and D), *exo84b-2* (B and E), and *trs120-4* (C and F).

(A–C) Single slices of FIB/SEM are shown on the left and 3D reconstructions of entire stacks on the right.

(B) Note the regular shape of the cell and the complete cross wall, as in the wild-type.

(C) Arrowhead points to the same cell wall gap in the micrograph (left) and 3D reconstruction (right). Arrows point to other gaps in the same cross wall. See Figure S4 for selected micrographs from the same series showing 3D reconstruction.

(D–F) TEMs. Arrowheads point to interphase nuclei, as evidenced by decondensed DNA (N) and a fully formed nuclear envelope (surrounded by a dotted white line). Note the complete cross walls in (D) and (E) and contrast this to the incomplete cross wall in (F; arrows), which has the appearance of beads on a string. Scale bars, 2 μm.

We compared the exocyst subunits with four other plasma membrane proteins: SYP121 and SYP122, and the auxin efflux carriers PIN1 and PIN2 (Collins et al., 2003; Assaad et al., 2004; Benková et al., 2003; Abas et al., 2006). In the wild-type, plasma membrane markers and polysaccharide stains labeled the cell plate, lateral walls, and cross wall compartments differentially (Figures 5A–5F; Figures S5D and S5E). In *club-2* mutants, by contrast, cell plates were labeled with equal relative intensity as the surrounding plasma membrane (Figures 5A–5E and 5G; Figures S5D and S5E). In other words, enrichment factors at the cell plate ranged from 9.5 to 0.3 in the wild-type, but oscillated around 1.0 in *club-2* (compare Figure 5F with Figure 5G). The

two markers most enriched at the cell plate in the wild-type, namely, JIM7 and SYP121-GFP, were almost completely absent at both the cell plate and plasma membrane or cell wall in *club-2* mutants (Figures 5A and 5E; Figure S5D). Taken together, the data show that *club/trs130* mutants appeared to have lost the ability to differentially exclude or target membrane proteins from or to the cell plate during different stages of cytokinesis.

appear to be perturbed in the *exo84b-2* mutant background (Figure S3D). By contrast, EXO84b-GFP had a dramatically altered, punctate appearance in the *club/trs130-2* mutant background (Figure 5D; Figure S5D). The features we invariably detected in the wild-type, namely, a clear membrane signal during cell plate initiation and cross wall maturation versus a diffuse cloud during cell plate expansion, were never seen in *club-2* mutants ($n = 100$ wild-type and $n = 130$ *club-2* seedlings). Enrichment factors at expanding cell plates (signal intensity at the cell plate compared to the signal at the plasma membrane and as normalized against FM4-64 values; see Experimental Procedures) were significantly different between the wild-type and *club-2* ($p = 0.004$; Figures 5F and 5G; Figure S5D). This suggests that the TRAPP11 complex may, directly or indirectly, be required to target the exocyst to cell plate initials and to maturing cell plates at the onset and end of cytokinesis. It is tempting to speculate that it might also be required to sort the exocyst away from expanding cell plates during the juvenile phase of cytokinesis.

The TRAPP11 and Exocyst Complexes Physically Interact

The colocalization of the TRAPP11 and exocyst complexes at key transitions at the beginning and end of cytokinesis as well as the dependence of exocyst localization on TRAPP11 function prompted us to ask whether the two tethering complexes physically interact. The TRAPP11 complex consists of nine conserved subunits encoded by ten genes, and the exocyst complex of eight subunits encoded by 36 genes in *Arabidopsis*. To gauge which subunits might interact, we carried out anti-GFP pull-downs of CLUB-GFP and TRS120-GFP fusions in planta and identified

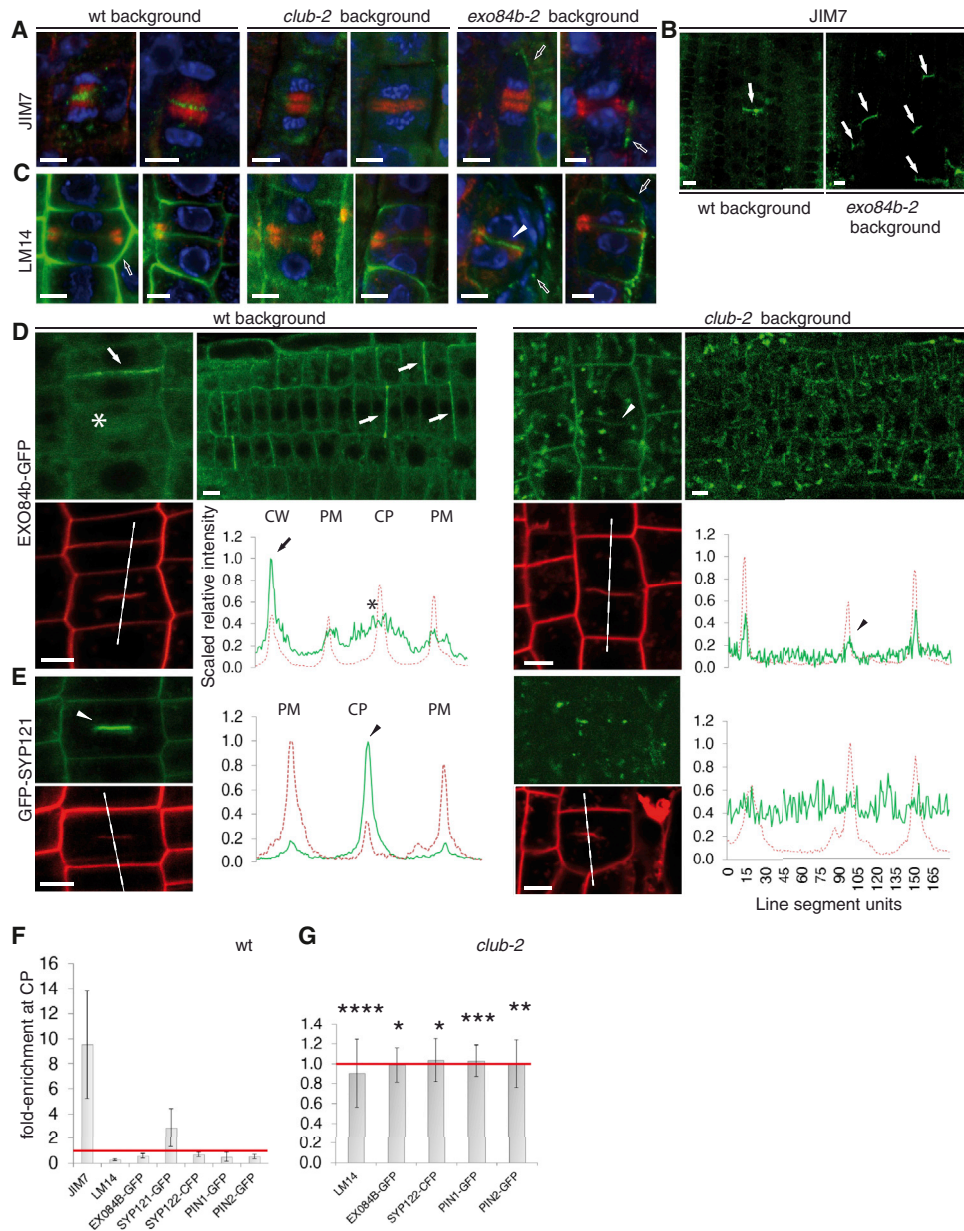


Figure 5. Cell Wall Polysaccharides and Protein Sorting at the Cell Plate

(A–C) Cell wall polysaccharide stains in root tips: DAPI/nucleus (blue), microtubules (red), and JIM7 or LM14 (green). (A) JIM7 antibody stain. In the wild-type (two left panels), JIM7-positive staining was detected on 97% of cell plates (n = 127). In *club-2* (middle panels), JIM7 staining was absent in 94% of cell plates (n = 68), and in *exo84b-2* (right panels) it was absent from 79% of cell plates (n = 33), but was often detected on lateral walls (white-rimmed black arrow). (B) Overviews of root tips showing ectopic cross wall stain (arrows) in *exo84b-2* mutants. These were more than 10-fold more frequent in the mutant than in the wild-type, in which a rare event is shown. (C) LM14 antibody stain. In the wild-type (two left panels), LM14-positive staining was weak or absent in 83% of expanding cell plates (n = 88). In *club-2* (middle panels), LM14 staining was present as of the ring-shaped phragmoplast in 67% of cell plates (n = 12); the stain was often punctate at the cell wall, and cell plates were labeled with the same intensity as lateral and cross walls. In *exo84b-2* (right panels) the stain was often punctate on lateral walls (white-rimmed black arrows; n = 7) and could be seen on nascent cross walls (arrow; n = 6). (D and E) Protein sorting at the cell plate. Left panels represent the wild-type and right panels *club-2* mutant backgrounds. The line graphs depict scaled relative fluorescence intensity, with FM4-64 (red) used to position the PM, CP, and the CW (arrow). (D) P_{EXO84b}::EXO84b-GFP. Asterisk indicates a cloud in the wild-type (left) and the arrowhead a small peak *club-2* (right); earlier time points show the same localization pattern. (E) P_{SYP121}::GFP-SYP121. Scale bars, 5 μm. (F and G) Fold-enrichment at the cell plate (compared to PM or CW) in the wild-type (F) and *club-2* (G). Mean ± SD and n ≥ 10 cells, with the following exceptions in (G): n = 5 for EXO84b, n = 5 for SYP122, and n = 8 for PIN1; see [Supplemental Experimental Procedures](#). *p < 0.005, **p < 0.001, ***p < 0.0001, and ****p < 0.00001 (Student's t test). See also [Figures S3](#) and [S5](#).

the purified proteins by mass spectrometry. This approach yielded ten hits including at least one isoform of each exocyst subunit (Figures 6A and 6B; Figure S6; Table S1). Western blots of the CLUB-GFP and AtTRS120-GFP pull-downs with antibodies against the exocyst subunits EXO84b, EXO70A1, and SEC6 confirmed an interaction between the TRAPP11 and exocyst complexes (Figure S7A). In an independent approach, a yeast two-hybrid screen with EXO70H7 as a bait identified AtTRS120, which documents a direct physical interaction between these subunits of the two tethering complexes (Figure S7B). We conclude that the TRAPP11 and exocyst complexes physically interact.

An analysis of the proteomics data suggests that only a small pool of the TRAPP11 bait interacts with exocyst components. This can be seen by the clustering of the two complexes in scatter plots, with the TRAPP11 components consistently having a higher intensity than the exocyst components (Figure 6A; Figure S6A). This could simply be due to a looser association between the two complexes than within a single complex, which would differentially affect the disruption of protein complexes during sample preparation. If the TRAPP11 and exocyst were to form a stoichiometric complex in plant cells, however, one might predict that TRAPP11 and exocyst mutants would have similar phenotypes, which is not the case. Rather, we observed salient differences between TRAPP11 and exocyst mutants: TRAPP11 mutants had canonical cytokinesis defects, including bloated cells and incomplete walls (Figures 6D and 6E), whereas *exo84b-2* had a cell wall-related defect, namely, broken walls in vacuolate cells (Fendrych et al., 2010), radial swelling, and isodiametric in lieu of elongated cells, for example in the hypocotyl (Figures 6D and 6G). These features are characteristic of cell wall mutants such as *procuste* and *rsw1* (Fagard et al., 2000; Peng et al., 2000). As the TRAPP11 and exocyst subunits do not colocalize in nondividing cells (other than the cytosolic pools; Figure S3C) and only transiently colocalize in dividing cells, the data are consistent with a model whereby the two complexes would transiently interact during key transitions at the onset and end of cytokinesis.

DISCUSSION

Our data support a model for the sequential, yet overlapping, coordinated action of the TRAPP11 and exocyst complexes in the regulation of plant cytokinesis (Figure 7). Plant cytokinesis can be broken down into four stages: initiation, biogenesis, expansion, and maturation (Figure 7). At the end of cytokinesis, the cell plate has matured into a cross wall flanked on either side by plasma membranes. Based on their localization patterns, we speculate that the TRAPP11 and exocyst complexes coordinate the spatiotemporal regulation of cell plate initiation. Thereafter, the TRAPP11 complex gives the juvenile compartment a TGN identity and drives its rapid growth, whereas the exocyst mediates the maturation process that enables the transition from TGN to plasma membrane identity (Figure 7). We propose that this switch in membrane identity drives the observed changes in polysaccharide composition, because the tethering complexes would tether different vesicle populations carrying different cargo to the cell plate or cross wall. Coordination between the complexes is implicated by the observation that

the TRAPP11 complex sorts the exocyst complex at the cell plate, and by the physical interaction between the complexes. We refer to this model as a “relay race” model, in which two protein complexes act as players in a relay race, each having a different role (as in being responsible for a different lap), and interacting transiently to coordinate transitions (as in passing the buck to each other between laps).

The strong initial signal at the cell plate seen with all exocyst subunits during the phragmoplast assembly stage raises the question as to the role of the exocyst in the initiation of cytokinesis. Electron tomographs of this stage document vesicles tethered by Y-shaped complexes that strongly resemble the exocyst as well as dumbbell-shaped cell plate precursors arising from initial fusion events (Seguí-Simarro et al., 2004; Figure 7). Interestingly, Fendrych et al. (2010) detected aberrant, donut-shaped FM4-64-positive membranes at the equator of root tips cells of *exo70a1* mutants at the onset of cytokinesis, but normal cell plates at later stages. A recent study in budding yeast has shown that the assembly of the exocyst is inhibited during mitosis by the cell-cycle-dependent phosphorylation of Exo84p (Luo et al., 2013). This provides a very interesting link between cell-cycle progression and membrane traffic during mitosis. To avoid bisecting the nucleus, this level of coordination is also required for the initiation of plant cytokinesis, and it will be interesting to see whether this is mediated by the exocyst.

A role for the TRAPP11 complex in cell plate biogenesis is substantiated by patchy or incomplete plates and cross walls we detected with TEM, SEM, and confocal microscopy. Consistently, the TRAPP11 complex was invariably associated with rapidly expanding regions, initially at the center and at later stages of the cell cycle at the leading edges of the cell plate. Although EXO84b does not appear to be required for cell plate formation, three lines of evidence suggest that it may play a role in cell plate maturation. First, the exocyst localized to the insertion site (Fendrych et al., 2010) and to areas of the cell plate that had already expanded. Second, we observed premature removal of KNOLLE from telophase plates in *exo84b-2*. This phenotype cannot readily be attributed to a general membrane recycling defect, as FM4-64 and TRS120 dynamics in the *exo84b-2* did not differ from that of the wild-type. The loss of KNOLLE as a juvenile trait can be considered as a first important step in the maturation of the cell plate into a cross wall, and its removal is an active process that is likely to require the action of the ESCRT complex (Spitzer et al., 2009). A third line of evidence was the altered relative content of methyl-esterified pectins and of AGP glycans in the cell plates, cross walls, and lateral walls of *exo84b-2* mutant root tips. Pectins are synthesized in the Golgi and deposited in the cell wall in a highly esterified form; in the cell wall, they undergo demethylesterification via a set of enzymes referred to as pectin methylesterases (PMEs) (Clausen et al., 2003). Our observation of JIM7-positive staining at the cell plate throughout cytokinesis supports the view that the cell plate is derived from Golgi/TGN- rather than endocytotic vesicles. This is discrepant with reports from Dhonukshe et al. (2006), but consistent with the observations of Chow et al. (2008). The absence of JIM7-positive staining in *club/trs130* mutant cell plates is yet another line of evidence for a role of the TRAPP11 complex in cell plate biogenesis. The ectopic JIM7 staining seen in lateral and cross walls in

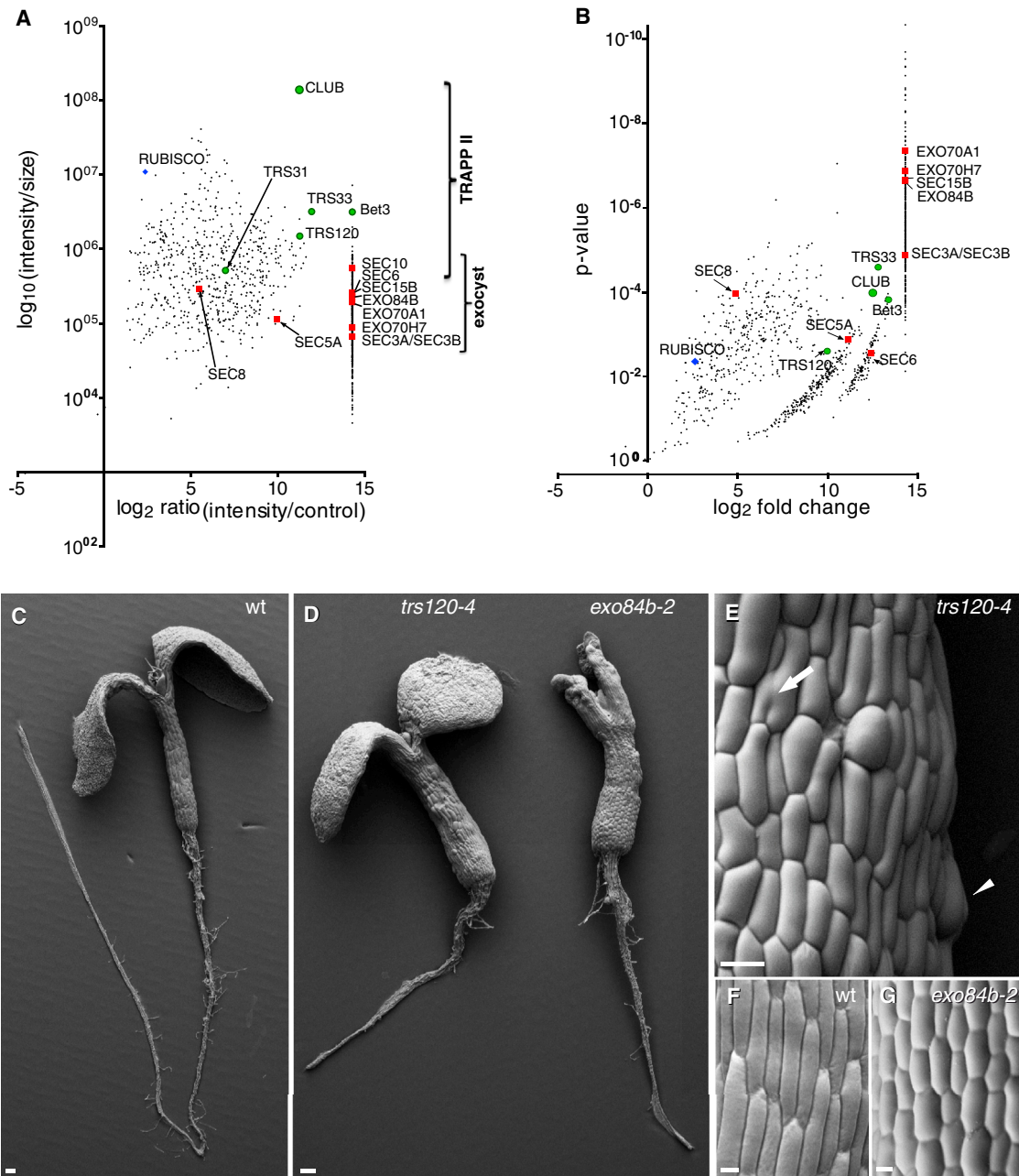


Figure 6. Physical Interaction between the TRAPP II and Exocyst Complexes and Mutant Phenotypes

(A and B) Scatter plots showing all the copurified proteins in a CLUB-GFP immunoprecipitate. Each protein is represented by at least five unique peptides and was present in all three biological replicates. The ratio was calculated for each protein as the intensity of the signal in the experiment divided by its intensity in the soluble GFP empty vector control. Green circles, TRAPP II subunits; red squares, exocyst subunits; blue diamond, rubisco.

(A) Signal intensity (normalized against protein size, \log_{10} scale) against the signal ratio (\log_2 scale). The CLUB-GFP bait has the highest intensity, as expected. An artificial line is formed to the right for proteins that had no signal in the control; these were attributed a random value so as not to appear at infinity on the plot. Rubisco is the most abundant protein in plant tissues and was found in the experiment and control at relatively comparable intensities (low \log_2 ratio). Note that TRAPP II subunits have a higher average signal intensity than exocyst subunits.

(B) The p value (Student's t test; depicted along a negative \log_{10} scale, but labeled with actual values) is plotted against the signal ratio. Note that a large number of exocyst components have lower p values than the actual bait, due to the fact that they had no signal in the empty vector control. Shown are hits with $p < 0.02$.

(C–G) SEMs of seedlings. (C and D) Overviews. (E–G) Close-ups. (C and F) Wild-type. (D, left; and E) *trs120-4*. In (E) the arrow points to a cell wall stub and the arrowhead to a bloated cell. (D, right; and G) *exo84b-2*. Scale bars, 100 μm (C and D); 20 μm (E–G).

See also [Figures S6](#) and [S7](#).

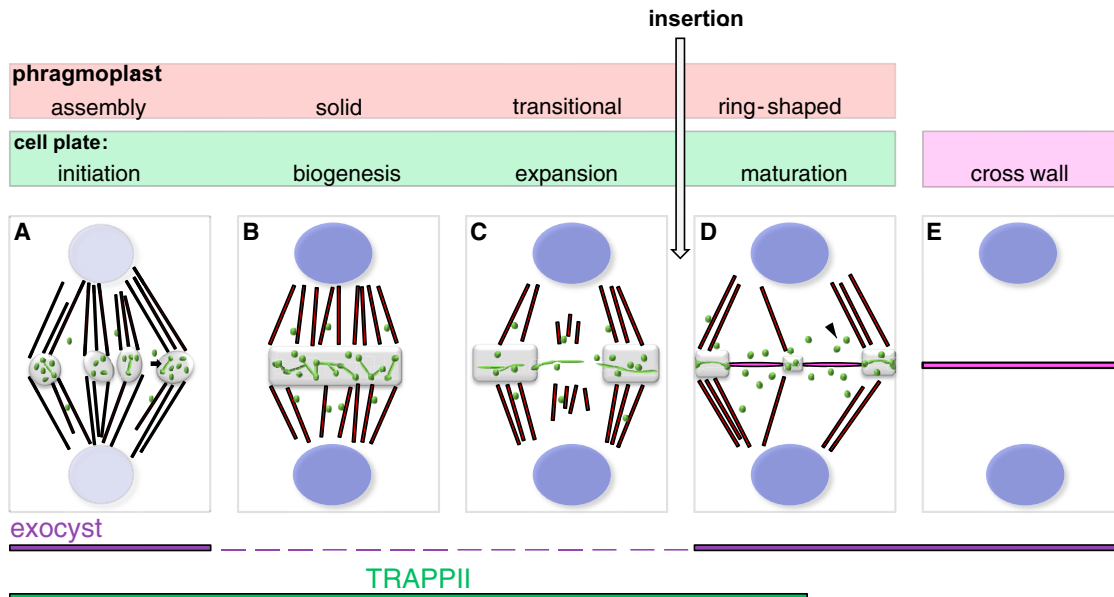


Figure 7. “Relay Race” Model for the Sequential but Overlapping and Coordinated Action of the TRAPP11 and Exocyst Complexes

Cytokinesis is broken down into four stages (top, A–D; adapted from Seguí-Simarro et al., 2004 with permission from the American Society of Plant Biologists). (A) The phragmoplast is assembled from opposite sets of polar spindle microtubules (red rod-like structures). A first round of vesicle fusion gives rise to dumbbell-shaped cell plate initials (arrow).

(B) At the solid phragmoplast stage, cell plate biogenesis occurs within a cell plate assembly matrix (CPAM; gray) via further rounds of membrane fusion.

(C) Cell plate expansion is driven by the reorganization of phragmoplast microtubules and membrane addition at the leading edges of the cell plate.

(D) Insertion occurs once the expanding cell plate has reached the parental walls. This event triggers maturation, which is accompanied by the loss of juvenile traits, including the removal of KNOLLE from cell plate membranes (arrowheads).

(E) At the end of cytokinesis, the cell plate has matured into a cross wall (fuchsia) flanked on either side by plasma membranes (black contour lines).

Bottom: We postulate that the TRAPP11 (dark green bar) and exocyst (purple bars) complexes are both required for the initiation of cytokinesis. Thereafter, the TRAPP11 complex drives cell plate biogenesis and expansion, and the exocyst complex appears to be required for cell plate maturation (see text for details). Red, phragmoplast microtubules; green, cell plate membranes; pink, mature cell plates and cross wall; blue, nuclei (light blue, dividing nuclei); gray, CPAM.

exo84b-2 could reflect a deficiency in cell wall PMEs, or a general defect in pectin recycling from mother cell walls.

In addition to a role in cell plate biogenesis, we show in this study that the TRAPP11 complex is required for protein sorting at the cell plate. We monitored the localization dynamics of five plasma membrane proteins as well as the presence of a variety of cell wall polysaccharides in the cell plates of wild-type versus *club/trs130* root tips. Contrary to the view that the cell plate acts as a sink for plasma membrane proteins expressed during cytokinesis (Müller et al., 2003), we found that the dozen markers we monitored were differentially localized to the cell plate, plasma membrane, newly formed cross walls, or mature cell walls in the wild-type. By contrast, *club/trs130* mutants appeared to have lost the ability to distinguish between these compartments: the default localization pattern for the membrane or polysaccharide markers we imaged was that they accumulated in intracellular compartments and that they labeled the cell plate with roughly equal relative intensity as the plasma membrane or cross/lateral walls. Mislocalization cannot readily be attributed to cell plate aberrations in *club/trs130* mutants, seeing as we chose among mutant plates ones that had a fairly normal appearance on the basis of FM4-64 staining. Furthermore, sorting did not appear to be affected in other cytokinesis-defective mutants of similar overall appearance (K.R. and F.F.A., unpublished data). A trivial explanation would be that trafficking to

the plasma membrane requires prior passage through the TGN, which is a TRAPP11 compartment, and that plasma membrane proteins merely accumulate in an endomembrane compartment in TRAPP11 mutants; TRAPP11 mutants of *Arabidopsis* have in fact been shown to be impaired in Golgi transport to the cell wall (Qi et al., 2011). Although we cannot formally exclude this explanation, we do not feel that it accounts for the highly differential sorting we observed at the cell plate. Of nine plasma membrane markers, for example, the five exocyst subunits were the only ones to be present as a diffuse cloud around the cell plate during the anaphase-telophase transition, yet enriched at cross wall membranes during telophase (see also Fendrych et al., 2010; Zhang et al., 2013). This specific pattern was disrupted in *club/trs130* mutants, as were all other differential localization patterns. Taken together, our data suggest that the TRAPP11 complex is required not only for the biogenesis of the cell plate but also for its identity as a transient compartment distinct from newly formed cross walls and mature parental walls.

The *Arabidopsis* ECHIDNA protein is also involved in protein sorting at the cell plate (Gendre et al., 2011). ECHIDNA is thought to be required for the genesis of secretory vesicles at the TGN, and, accordingly, for the secretion of cell wall polysaccharides and for the deposition of de novo-synthesized membrane proteins such as the auxin influx carrier AUX1 at the plasma

membrane (Boutté et al., 2013; Gendre et al., 2013; McFarlane et al., 2013). The trafficking of the auxin efflux carrier PIN3 to the plasma membrane, however, does not require ECHIDNA function (Boutté et al., 2013). Similarly, the TRAPP11 complex is required for the polar localization of AUX1 and PIN2, but not PIN1, in root tips (Qi et al., 2011; Qi and Zheng, 2011). These observations highlight the differential regulation of trafficking to the plasma membrane as well as the highly sophisticated nature of post-Golgi trafficking in plants. It will be interesting to see whether ECHIDNA and the TRAPP11 complex act in concert and/or in parallel to regulate the diverse functions of the plant TGN.

We postulate that the sequential, coordinated action of the TRAPP11 and exocyst complexes may also be required for the spatiotemporal regulation of cytokinesis in fungi and in animals. Mutations in the *bru* gene of *Drosophila*, a TRAPP11-specific Trs120 ortholog, specifically cause failure of cleavage furrow ingression (Robinett et al., 2009). Rab11 localization to the cleavage furrow depends on *bru*, and *bru* and Rab11 interact genetically (Robinett et al., 2009). Although the TRAPP11 complex may be required for cleavage furrow ingression, the exocyst appears to be required at the terminal phase of cytokinesis, namely, at the midbody for secretory vesicle-mediated abscission (Gromley et al., 2005; Neto et al., 2013; reviewed by Neto and Gould, 2011). Similarly, in fission yeast exocyst mutants are not defective at early stages of cytokinesis, which include actomyosin ring and division septum assembly, but are specifically impaired in cell separation at the end of cytokinesis (Wang et al., 2002). The exocyst targets hydrolytic enzymes to the septum that in turn digest the primary septum and surrounding wall and thereby enable cell separation (Martín-Cuadrado et al., 2005).

Although cell plate assembly and maturation in plants versus contractile ring and midbody assembly and function in animals comprise very different strategies for cytokinesis, there are some interesting common ancestral components. In the primitive red alga *Cyanidium caldarium* RK-1, for example, cytokinesis occurs by means of a contractile ring (Suzuki et al., 1995). Also, in the alga *Spirogyra* cytokinesis is initiated by a cleavage furrow and completed via a cell plate (McIntosh et al., 1995). Conversely, somatic cytokinesis in higher plants can be considered to be initiated by a cell plate and completed by a centripetal (from the outside in, like the furrow) process (Van Damme et al., 2011). Indeed, cell plate anchoring and insertion into the lateral walls occur via a TGN-independent centripetal recruitment pathway (Van Damme et al., 2011). Regardless of evolutionary considerations, however, we suggest that, across kingdoms, the TRAPP11 complex is required to mediate membrane addition during an initial growth phase of cytokinesis, and the exocyst later during cytokinesis for cell separation.

We have suggested a model whereby key transitions in membrane identity and function are mediated by the sequential yet overlapping and coordinated action of two tethering complexes. The cell plate is a transient compartment that, once cytokinesis is completed, matures into a cross wall, flanked on either side by plasma membranes. While the predominant role of the cell plate is growth, the cell wall lends the plant cell positional information, support, and tensile strength, and the plasma membrane represents a highly regulated interface between the inner and outer surfaces of plant cells. Thus, the

cell plate is an interesting example of a membrane compartment whose composition and function change as it undergoes biogenesis, expansion, and maturation. There are many other examples for which this is the case. Upon fungal infection, for example, a feeding structure called the haustorium is formed. The haustorium is surrounded by an extrahaustorial membrane, which is contiguous with but distinct from the host plasma membrane (Koh et al., 2005). It will be interesting to see whether the model of sequential coordinated action by two different tethering complexes can be applied to situations other than cytokinesis in which membrane identity and function are sequentially regulated in time and space.

EXPERIMENTAL PROCEDURES

Lines and Growth Conditions

Due to their seedling lethality, mutant lines were propagated as hetero- or hemi-zygotes. Insertion lines were selected via the TAIR and NASC websites (Swarbreck et al., 2008). Plants were grown in the greenhouse throughout the year, under controlled temperature conditions and with supplemental light, or under controlled growth chamber conditions (16/8 hr photoperiod at 250 $\mu\text{mol m}^{-2}\text{s}^{-1}$). Seedlings were surface sterilized, stratified at 4°C for 2 days, and plated on Murashige and Skoog medium supplemented with 1% sucrose and B5 vitamins (Sigma). The root tips of 5-day-old plate-grown seedlings were used for light, confocal, and electron microscopies.

Antibody Stains and Confocal Microscopy

Antibody stains were carried out as described by Völker et al. (2001), with anti-KNOLLE (rabbit, 1:2,000; Lauber et al., 1997), anti-tubulin (mouse, 1:2,500; Sigma), JIM7 (rat monoclonal, 1:10; Carbosource), and LM14 (rat monoclonal, 1:10; PlantProbes). Secondary antibodies are described in the Supplemental Experimental Procedures. Nuclei were stained with 1 mg/ml DAPI (Sigma). A Fluoview 1000 confocal laser scanning microscope (Olympus) was used as well as a CSU-X1 Yokogawa spinning disk head fitted to a Nikon Ti-E inverted microscope.

Electron Microscopy

For SEM of fresh material, samples were placed onto stubs and examined immediately in low vacuum with a Zeiss (LEO) VP 438 scanning electron microscope operated at 15 kV. Electron micrographs were digitally recorded from the backscattered electron-signal. For electron microscopy, root tips were placed in aluminum platelets, infiltrated with BSA, and fixed by high-pressure freezing (Leica Microsystems HPM100 system). Freeze substitution was performed in acetone with 2% osmium tetroxide and 0.2% uranyl acetate, including 5% water. The FIB serial sectioning was performed using a Zeiss-Auriga workstation. FIB/SEM tomographic data sets were obtained via the “slice and view” technique using a Zeiss Auriga 60 dual-beam instrument. A Zeiss EM912 Omega transmission electron microscope was used for TEM.

Coimmunoprecipitation

Coimmunoprecipitation experiments were carried out on 3 g of inflorescences using GFP-trap beads (Chromotek), as described by Park et al. (2012), with the following modifications: we supplemented both the lysis and washing buffers with a protease inhibitor cocktail for plants (Sigma-Aldrich P9599) and added 1 mM phenylmethanesulfonyl fluoride every 45 min. An inhibitor of proteasome activity (Sigma-Aldrich C2211) was also added to the lysis buffer. The washing buffer (50 mM Tris [pH 7.5] and 0.2% [v/v] Triton X-100) was supplemented with 200 mM NaCl. Cell fractionation, mass spectrometry, peptide and protein identification, data analysis, and western blot procedures are described in the Supplemental Experimental Procedures.

Statistics and Image Analysis

The *p* values were determined with the Student's two-tailed *t* test and set at a cutoff of 2%. Images were processed with Adobe Photoshop and assembled with Adobe Illustrator. 3D reconstructions were carried out with Imaris software (Bitplane). Images were analyzed with ImageJ (NIH). Line graphs of

mean signal intensities (Figure 2) were corrected for photobleaching during the course of a time lapse. Enrichment factors (Figure 5) were computed as mean signal intensity at the cell plate divided by the mean signal intensity at the plasma membrane or cell wall. For the plasma membrane markers, these values were normalized against FM4-64 cell plate/plasma membrane intensities. The entire cell plate and surrounding plasma membrane or cell wall were traced, where these were clearly delineated; these criteria excluded JIM7 and SYP121 in *club-2* mutants as these had a punctate appearance and failed to label either the cell plate or the cell wall/plasma membrane compartments. We used at least ten cells per measurement in the wild-type, but in *club-2* mutants the sample size was lower in three cases (see figure legend). This is due to the difficulty of detecting cell plates in a mutant with a low mitotic index that is impaired in cell plate biogenesis and FM4-64 uptake. Thus, in the case of EXO84b-GFP, we were only able to detect five cell plates in 130 mutant seedlings.

SUPPLEMENTAL INFORMATION

Supplementary Information includes Supplemental Experimental Procedures, seven figures, one table, and three movies and can be found with this article online at <http://dx.doi.org/10.1016/j.devcel.2014.04.029>.

ACKNOWLEDGMENTS

We thank Prof. Grill and members of the Botany Department for support. Silvia Dobler helped with sample preparation. Matyas Fendrych prepared the EXO84b antibody. Alex Ivakov helped with spinning disk confocal microscopy. Ngoc Nguyen provided technical assistance. We thank TAIR and NASC for insertion lines. Thanks to Heather McFarlane for useful suggestions and a critical evaluation of the manuscript. We are grateful to Eva Benkova and Christian Luschignig for sharing published resources. Distribution of the JIM7 antibody was supported in part by NSF grant DBI-0421683 and RCN 009281. K.R. and A.S. were supported by DFG grants AS110/4-6 and AS110/5-1; L.S. and V.Z. by Czech Science Foundation grants GPP501/11/P853 and GACR P305/11/1629, respectively; and I.K. by a Charles University grant (Prague project 658112). S.P. was funded by the Max Planck Gesellschaft. This research was funded by DFG grants to F.F.A. and G.W.

Received: August 2, 2013

Revised: February 13, 2014

Accepted: April 25, 2014

Published: May 29, 2014

REFERENCES

- Abas, L., Benjamins, R., Malenica, N., Paciorek, T., Wiśniewska, J., Moulinier-Anzola, J.C., Sieberer, T., Friml, J., and Luschignig, C. (2006). Intracellular trafficking and proteolysis of the Arabidopsis auxin-efflux facilitator PIN2 are involved in root gravitropism. *Nat. Cell Biol.* 8, 249–256.
- Assaad, F.F., Qiu, J.L., Youngs, H., Ehrhardt, D., Zimmerli, L., Kalde, M., Wanner, G., Peck, S.C., Edwards, H., Ramonell, K., et al. (2004). The PEN1 syntaxin defines a novel cellular compartment upon fungal attack and is required for the timely assembly of papillae. *Mol. Biol. Cell* 15, 5118–5129.
- Benková, E., Michniewicz, M., Sauer, M., Teichmann, T., Seifertová, D., Jürgens, G., and Friml, J. (2003). Local, efflux-dependent auxin gradients as a common module for plant organ formation. *Cell* 115, 591–602.
- Boutté, Y., Jonsson, K., McFarlane, H.E., Johnson, E., Gendreau, D., Swarup, R., Friml, J., Samuels, L., Robert, S., and Bhalerao, R.P. (2013). ECHIDNA-mediated post-Golgi trafficking of auxin carriers for differential cell elongation. *Proc. Natl. Acad. Sci. USA* 110, 16259–16264.
- Chow, C.-M., Neto, H., Foucart, C., and Moore, I. (2008). Rab-A2 and Rab-A3 GTPases define a trans-golgi endosomal membrane domain in Arabidopsis that contributes substantially to the cell plate. *Plant Cell* 20, 101–123.
- Clausen, M.H., Willats, W.G., and Knox, J.P. (2003). Synthetic methyl hexagalacturonate hapten inhibitors of anti-homogalacturonan monoclonal antibodies LM7, JIM5 and JIM7. *Carbohydr. Res.* 338, 1797–1800.
- Collins, N.C., Thordal-Christensen, H., Lipka, V., Bau, S., Kombrink, E., Qiu, J.L., Hüchelhoven, R., Stein, M., Freialdenhoven, A., Somerville, S.C., and Schulze-Lefert, P. (2003). SNARE-protein-mediated disease resistance at the plant cell wall. *Nature* 425, 973–977.
- Cutler, S.R., and Ehrhardt, D.W. (2002). Polarized cytokinesis in vacuolate cells of Arabidopsis. *Proc. Natl. Acad. Sci. USA* 99, 2812–2817.
- Cvrckova, F., Elias, M., Hala, M., Obermeyer, G., and Zarsky, V. (2001). Small GTPases and conserved signalling pathways in plant cell morphogenesis: from exocytosis to the exocyst. In *Cell Biology of Plant and Fungal Tip Growth*, A. Geitmann, M. Cresti, and I.B. Heath, eds. (Amsterdam: IOS Press), pp. 105–122.
- Dhonukshe, P., Baluska, F., Schlicht, M., Hlavacka, A., Samaj, J., Friml, J., and Gadella, T.W., Jr. (2006). Endocytosis of cell surface material mediates cell plate formation during plant cytokinesis. *Dev. Cell* 10, 137–150.
- Fagard, M., Desnos, T., Desprez, T., Goubet, F., Refregier, G., Mouille, G., McCann, M., Rayon, C., Vernhettes, S., and Höfte, H. (2000). PROCUSTE1 encodes a cellulose synthase required for normal cell elongation specifically in roots and dark-grown hypocotyls of Arabidopsis. *Plant Cell* 12, 2409–2424.
- Fendrych, M., Synek, L., Pecenkova, T., Toupalova, H., Cole, R., Drdova, E., Nebesarova, J., Sedinova, M., Hala, M., Fowler, J.E., and Zarsky, V. (2010). The Arabidopsis exocyst complex is involved in cytokinesis and cell plate maturation. *Plant Cell* 22, 3053–3065.
- Fendrych, M., Synek, L., Pecenkova, T., Drdova, E.J., Sekeres, J., de Rycke, R., Nowack, M.K., and Zarsky, V. (2013). Visualization of the exocyst complex dynamics at the plasma membrane of Arabidopsis thaliana. *Mol. Biol. Cell* 24, 510–520.
- Gendreau, D., Oh, J., Boutté, Y., Best, J.G., Samuels, L., Nilsson, R., Uemura, T., Marchant, A., Bennett, M.J., Grebe, M., and Bhalerao, R.P. (2011). Conserved Arabidopsis ECHIDNA protein mediates trans-Golgi-network trafficking and cell elongation. *Proc. Natl. Acad. Sci. USA* 108, 8048–8053.
- Gendreau, D., McFarlane, H.E., Johnson, E., Mouille, G., Sjödin, A., Oh, J., Levesque-Tremblay, G., Watanabe, Y., Samuels, L., and Bhalerao, R.P. (2013). Trans-Golgi network localized ECHIDNA/Ypt interacting protein complex is required for the secretion of cell wall polysaccharides in Arabidopsis. *Plant Cell* 25, 2633–2646.
- Gromley, A., Yeaman, C., Rosa, J., Redick, S., Chen, C.-T., Mirabelle, S., Guha, M., Sillibourne, J., and Doxsey, S.J. (2005). Centriolin anchoring of exocyst and SNARE complexes at the midbody is required for secretory-vesicle-mediated abscission. *Cell* 123, 75–87.
- Gutierrez, R., Lindeboom, J.J., Paredes, A.R., Emons, A.M.C., and Ehrhardt, D.W. (2009). Arabidopsis cortical microtubules position cellulose synthase delivery to the plasma membrane and interact with cellulose synthase trafficking compartments. *Nat. Cell Biol.* 11, 797–806.
- Heider, M.R., and Munson, M. (2012). Exorcising the exocyst complex. *Traffic* 13, 898–907.
- Jaber, E., Thiele, K., Kindziński, V., Loderer, C., Rybak, K., Jürgens, G., Mayer, U., Söllner, R., Wanner, G., and Assaad, F.F. (2010). A putative TRAPP11 tethering factor is required for cell plate assembly during cytokinesis in Arabidopsis. *New Phytol.* 187, 751–763.
- Koh, S., André, A., Edwards, H., Ehrhardt, D., and Somerville, S. (2005). Arabidopsis thaliana subcellular responses to compatible Erysiphe cichoracearum infections. *Plant J.* 44, 516–529.
- Lauber, M.H., Waizenegger, I., Steinmann, T., Schwarz, H., Mayer, U., Hwang, I., Lukowitz, W., and Jürgens, G. (1997). The Arabidopsis KNOLLE protein is a cytokinesis-specific syntaxin. *J. Cell Biol.* 139, 1485–1493.
- Luo, G., Zhang, J., Luca, F.C., and Guo, W. (2013). Mitotic phosphorylation of Exo84 disrupts exocyst assembly and arrests cell growth. *J. Cell Biol.* 202, 97–111.
- Martín-Cuadrado, A.B., Morrell, J.L., Konomi, M., An, H., Petit, C., Osumi, M., Balasubramanian, M., Gould, K.L., Del Rey, F., and de Aldana, C.R. (2005). Role of septins and the exocyst complex in the function of hydrolytic enzymes responsible for fission yeast cell separation. *Mol. Biol. Cell* 16, 4867–4881.
- McFarlane, H.E., Watanabe, Y., Gendreau, D., Carruthers, K., Levesque-Tremblay, G., Haughn, G.W., Bhalerao, R.P., and Samuels, L. (2013). Cell

- wall polysaccharides are mislocalized to the Vacuole in *echidna* mutants. *Plant Cell Physiol.* **54**, 1867–1880.
- McIntosh, K., Pickett-Heaps, J.D., and Gunning, B.E.S. (1995). Cytokinesis in Spirogyra: Integration of Cleavage and Cell-Plate Formation. *Int. J. Plant Sci.* **156**, 1–8.
- McMichael, C.M., and Bednarek, S.Y. (2013). Cytoskeletal and membrane dynamics during higher plant cytokinesis. *New Phytol.* **197**, 1039–1057.
- Mineyuki, Y., and Gunning, B.E.S. (1990). A role for preprophase bands of microtubules in maturation of new cell walls, and a general proposal on the function of the preprophase band sites in cell division in higher plants. *J. Cell Sci.* **97**, 527–537.
- Moller, I., Marcus, S.E., Haeger, A., Verhertbruggen, Y., Verhoef, R., Schols, H., Ulvskov, P., Mikkelsen, J.D., Knox, J.P., and Willats, W. (2008). High-throughput screening of monoclonal antibodies against plant cell wall glycans by hierarchical clustering of their carbohydrate microarray binding profiles. *Glycoconj. J.* **25**, 37–48.
- Moore, P.J., and Staehelin, L.A. (1988). Immunogold localization of the cell-wall-matrix polysaccharides rhamnogalacturonan I and xyloglucan during cell expansion and cytokinesis in *Trifolium pratense* L.; implication for secretory pathways. *Planta* **174**, 433–445.
- Müller, I., Wagner, W., Völker, A., Schellmann, S., Nacry, P., Küttner, F., Schwarz-Sommer, Z., Mayer, U., and Jürgens, G. (2003). Syntaxin specificity of cytokinesis in Arabidopsis. *Nat. Cell Biol.* **5**, 531–534.
- Neto, H., and Gould, G.W. (2011). The regulation of abscission by multi-protein complexes. *J. Cell Sci.* **124**, 3199–3207.
- Neto, H., Kaupisch, A., Collins, L.L., and Gould, G.W. (2013). Syntaxin 16 is a master recruitment factor for cytokinesis. *Mol. Biol. Cell* **24**, 3663–3674.
- Park, M., Touihri, S., Müller, I., Mayer, U., and Jürgens, G. (2012). Sec1/Munc18 protein stabilizes fusion-competent syntaxin for membrane fusion in Arabidopsis cytokinesis. *Dev. Cell* **22**, 989–1000.
- Peng, L., Hocart, C.H., Redmond, J.W., and Williamson, R.E. (2000). Fractionation of carbohydrates in Arabidopsis root cell walls shows that three radial swelling loci are specifically involved in cellulose production. *Planta* **211**, 406–414.
- Qi, X., and Zheng, H. (2011). Arabidopsis TRAPP^{II} is functionally linked to Rab-A, but not Rab-D in polar protein trafficking in trans-Golgi network. *Plant Signal. Behav.* **6**, 1679–1683.
- Qi, X., Kaneda, M., Chen, J., Geitmann, A., and Zheng, H. (2011). A specific role for Arabidopsis TRAPP^{II} in post-Golgi trafficking that is crucial for cytokinesis and cell polarity. *Plant J.* **68**, 234–248.
- Robinett, C.C., Giansanti, M.G., Gatti, M., and Fuller, M.T. (2009). TRAPP^{II} is required for cleavage furrow ingression and localization of Rab11 in dividing male meiotic cells of *Drosophila*. *J. Cell Sci.* **122**, 4526–4534.
- Samuels, A.L., Giddings, T.H., Jr., and Staehelin, L.A. (1995). Cytokinesis in tobacco BY-2 and root tip cells: a new model of cell plate formation in higher plants. *J. Cell Biol.* **130**, 1345–1357.
- Seguí-Simarro, J.M., Austin, J.R., 2nd, White, E.A., and Staehelin, L.A. (2004). Electron tomographic analysis of somatic cell plate formation in meristematic cells of Arabidopsis preserved by high-pressure freezing. *Plant Cell* **16**, 836–856.
- Söllner, R., Glässer, G., Wanner, G., Somerville, C.R., Jürgens, G., and Assaad, F.F. (2002). Cytokinesis-defective mutants of Arabidopsis. *Plant Physiol.* **129**, 678–690.
- Spitzer, C., Reyes, F.C., Buono, R., Sliwinski, M.K., Haas, T.J., and Otegui, M.S. (2009). The ESCRT-related CHMP1A and B proteins mediate multivesicular body sorting of auxin carriers in Arabidopsis and are required for plant development. *Plant Cell* **21**, 749–766.
- Suzuki, K., Kawazu, T., Mita, T., Takahashi, H., Itoh, R., Toda, K., and Kuroiwa, T. (1995). Cytokinesis by a contractile ring in the primitive red alga *Cyanidium caldarium* RK-1. *Eur. J. Cell Biol.* **67**, 170–178.
- Swarbreck, D., Wilks, C., Lamesch, P., Berardini, T.Z., Garcia-Hernandez, M., Foerster, H., Li, D., Meyer, T., Muller, R., Ploetz, L., et al. (2008). The Arabidopsis Information Resource (TAIR): gene structure and function annotation. *Nucleic Acids Res.* **36** (Database issue), D1009–D1014.
- Synek, L., Schlager, N., Eliás, M., Quentin, M., Hauser, M.-T., and Zárský, V. (2006). AtEXO70A1, a member of a family of putative exocyst subunits specifically expanded in land plants, is important for polar growth and plant development. *Plant J.* **48**, 54–72.
- Thellmann, M., Rybak, K., Thiele, K., Wanner, G., and Assaad, F.F. (2010). Tethering factors required for cytokinesis in Arabidopsis. *Plant Physiol.* **154**, 720–732.
- Thiele, K., Wanner, G., Kindzierski, V., Jürgens, G., Mayer, U., Pachi, F., and Assaad, F.F. (2009). The timely deposition of callose is essential for cytokinesis in Arabidopsis. *Plant J.* **58**, 13–26.
- Van Damme, D., Gadeyne, A., Vanstraelen, M., Inzé, D., Van Montagu, M.C., De Jaeger, G., Russinova, E., and Geelen, D. (2011). Adaptin-like protein TPLATE and clathrin recruitment during plant somatic cytokinesis occurs via two distinct pathways. *Proc. Natl. Acad. Sci. USA* **108**, 615–620.
- Völker, A., Stierhof, Y.D., and Jürgens, G. (2001). Cell cycle-independent expression of the Arabidopsis cytokinesis-specific syntaxin KNOLLE results in mistargeting to the plasma membrane and is not sufficient for cytokinesis. *J. Cell Sci.* **114**, 3001–3012.
- Wang, H., Tang, X., Liu, J., Trautmann, S., Balasundaram, D., McCollum, D., and Balasubramanian, M.K. (2002). The multiprotein exocyst complex is essential for cell separation in *Schizosaccharomyces pombe*. *Mol. Biol. Cell* **13**, 515–529.
- Wu, J., Tan, X., Wu, C., Cao, K., Li, Y., and Bao, Y. (2013). Regulation of cytokinesis by exocyst subunit SEC6 and KEULE in Arabidopsis thaliana. *Mol. Plant* **6**, 1863–1876.
- Yu, S., and Liang, Y. (2012). A trapper keeper for TRAPP, its structures and functions. *Cell. Mol. Life Sci.* **69**, 3933–3944.
- Yu, X., Prekeris, R., and Gould, G.W. (2007). Role of endosomal Rab GTPases in cytokinesis. *Eur. J. Cell Biol.* **86**, 25–35.
- Zhang, Y., Immink, R., Liu, C.-M., Emons, A.M., and Ketelaar, T. (2013). The Arabidopsis exocyst subunit SEC3A is essential for embryo development and accumulates in transient puncta at the plasma membrane. *New Phytol.* **199**, 74–88.